

Investigation of the effects of the graphene-substrate hybridization on the optical conductivity of graphene

Muhammad Aziz Majidi, Wileam Yonatan Phan', and Andrivo Rusydi

Citation: **1729**, 020016 (2016); doi: 10.1063/1.4946919

View online: <http://dx.doi.org/10.1063/1.4946919>

View Table of Contents: <http://aip.scitation.org/toc/apc/1729/1>

Published by the [American Institute of Physics](#)

Investigation of the Effects of the Graphene-Substrate Hybridization on the Optical Conductivity of Graphene

Muhammad Aziz Majidi^{1,2,3}, Wileam Yonatan Phan^{1,a)} and Andrivo Rusydi^{2,3}

¹*Departemen Fisika, FMIPA, Universitas Indonesia, Kampus UI Depok, Indonesia*

²*Singapore Synchrotron Light Source, National University of Singapore,*

5 Research Link, Singapore 117603, Singapore

³*NUSNNI-NanoCore, Department of Physics, National University of Singapore, Singapore 117576, Singapore*

^{a)}Corresponding author: wileam.yonatan@sci.ui.ac.id

Abstract. Graphene is an emerging two-dimensional material with a lot of promising applications as devices, in which it must be combined with other materials, most notably put on top of a substrate. Recent research has shown that certain substrates can change the physical properties of graphene dramatically. Here, we propose a simple model describing a system of single layer graphene on top of a layered insulating substrate based on the tight-binding approximation, where we introduce a hybridization term of the graphene $2p_z$ orbital and topmost substrate layer orbitals. We then calculate the density of states $DOS(\nu)$ and the real part of the optical conductivity tensor $\sigma_1^{ab}(\omega)$ of the graphene layer for various values of the substrate band gap. The results show that the graphene-substrate hybridization tends to create states around the Fermi energy, thus enhancing the DC conductivity of the graphene layer. Furthermore, the peak in the $\sigma_1^{aa}(\omega)$ of graphene tends to get renormalized and experience a redshift, most prominently when the substrate band gap matches twice the graphene nearest-neighbor hopping parameter t_g . Meanwhile, an insulating substrate with a very high band gap (around $4t_g$) weakens the effects of the hybridization.

INTRODUCTION

Ten years after graphene was successfully synthesized for the first time in 2004 [1], this fascinating two-dimensional material has started to find its applications in creating novel optoelectronic devices, e.g., ultra-sensitive photodetectors [2, 3, 4], nearly transparent solar cells [5, 6, 7, 8], flexible light emitting diodes [9], and so on. As graphene research continues to move in this direction, there is an inevitable need to understand the interactions between graphene and other materials incorporated in these devices, especially the substrate onto which the graphene layer is deposited. Due to the strong electronic correlations present in graphene [10], many interesting effects show up at the graphene-substrate interface, including charge transfer, dielectric screening, and hybridization with the substrate. The latter has been highlighted to be significant for a specific substrate in a recent experimental work [11]. In this work, we investigate the significance of this hybridization between graphene $2p_z$ orbitals and substrate orbitals in the topmost substrate layer, and how far the properties of the substrate can influence the optical properties of the graphene layer.

MODEL

We model our graphene-on-substrate system with the following Hamiltonian,

$$\hat{\mathcal{H}} = \hat{\mathcal{H}}_g + \hat{\mathcal{H}}_s + \hat{\mathcal{H}}_v. \quad (1)$$

The first term describes monolayer graphene within tight-binding approximation on the honeycomb lattice,

$$\hat{\mathcal{H}}_g = -t_g \sum_{\mathbf{k}} \left[\left(e^{ik_x a / \sqrt{3}} + 2 \cos\left(\frac{k_y a}{2}\right) e^{-ik_x a / (2\sqrt{3})} \right) \hat{a}_{\mathbf{k}}^\dagger \hat{b}_{\mathbf{k}} + \text{h.c.} \right], \quad (2)$$

where $\hat{a}_{\mathbf{k}}^\dagger$ ($\hat{b}_{\mathbf{k}}$) is the creation (annihilation) operator for a $2p_z$ electron with momentum \mathbf{k} in the A (B) sublattice of graphene, and t_g is the hopping parameter for graphene electrons. The second term describes a simple, M -layer thick, two-basis insulating substrate within tight-binding approximation on a NaCl-like lattice structure,

$$\mathcal{H}_s = \sum_{\mathbf{k}'} \sum_{j=1}^M \left\{ \epsilon_A \hat{A}_{\mathbf{k}',j}^\dagger \hat{A}_{\mathbf{k}',j} + \epsilon_B \hat{B}_{\mathbf{k}',j}^\dagger \hat{B}_{\mathbf{k}',j} + \epsilon_i(\mathbf{k}') \left[\hat{A}_{\mathbf{k}',j}^\dagger \hat{B}_{\mathbf{k}',j} + \hat{B}_{\mathbf{k}',j}^\dagger \hat{A}_{\mathbf{k}',j} \right] - t_i \left[\hat{A}_{\mathbf{k}',j}^\dagger \hat{B}_{\mathbf{k}',j\pm 1} + \hat{B}_{\mathbf{k}',j}^\dagger \hat{A}_{\mathbf{k}',j\pm 1} \right] + \text{h.c.} \right\} . \quad (3)$$

Here, $\hat{A}_{\mathbf{k}',j}^\dagger$ ($\hat{B}_{\mathbf{k}',j}$) creates (annihilates) an electron with momentum \mathbf{k}' at the A (B) sublattice of the substrate, in the j -th layer, t_i is the hopping parameter for electrons in the substrate, while $\epsilon_A = -\epsilon_B$ are the on-site energies for electrons at the A and B sublattices of the substrate, respectively, which values can be used to control the value of the substrate band gap. Here we take ϵ_B to be positive, such that the substrate band gap is symmetric with respect to the center of the energy axis. $\epsilon_i(\mathbf{k}') = -2t_i (\cos(k'_x a) + \cos(k'_y a))$ is the two-dimensional energy dispersion of each substrate layer. Finally, the last term describes the hybridization between the monolayer graphene and the topmost substrate layer,

$$\mathcal{H}_v = V \sum_{\mathbf{k}, \mathbf{k}'} \delta_{\mathbf{k}, \mathbf{k}'} \left(\hat{a}_{\mathbf{k}}^\dagger \hat{A}_{\mathbf{k},1} + \hat{a}_{\mathbf{k}}^\dagger \hat{B}_{\mathbf{k},1} + \hat{b}_{\mathbf{k}}^\dagger \hat{A}_{\mathbf{k},1} + \hat{b}_{\mathbf{k}}^\dagger \hat{B}_{\mathbf{k},1} + \text{h.c.} \right) , \quad (4)$$

where V represents the hybridization strength. Note that the presence of the Kronecker delta $\delta_{\mathbf{k}, \mathbf{k}'}$ in this hybridization term allows us to express the Hamiltonian operator in terms of only one momentum variable. Since we are more interested in the properties of the graphene layer, we arbitrarily choose our momentum vectors to be those within the first Brillouin zone (FBZ) of graphene.

METHOD

The Hamiltonian as stated in Equation (1) can be expressed using spinor notation as

$$\mathcal{H} = \hat{\Psi}^\dagger [H(\mathbf{k})] \hat{\Psi} , \quad (5)$$

where $[H(\mathbf{k})]$ is the Hamiltonian matrix of size $(2 + 2M) \times (2 + 2M)$, and $\hat{\Psi}$ ($\hat{\Psi}^\dagger$) is a column (row) vector consisting of all the involved annihilation (creation) operators. From the Hamiltonian matrix, we can then construct the Green function and spectral function matrices, respectively, as follows,

$$[G(\mathbf{k}, \nu \pm i0^+)] = [(\nu \pm i0^+) [I] - [H(\mathbf{k})]]^{-1} , \quad (6)$$

$$[A(\mathbf{k}, \nu)] = \frac{i}{2\pi} \{ [G(\mathbf{k}, \nu + i0^+)] - [G(\mathbf{k}, \nu - i0^+)] \} , \quad (7)$$

where ν is energy variable, and derive the Cartesian components of the velocity matrices,

$$[v_\lambda(\mathbf{k})] = \frac{\partial}{\partial k_\lambda} [H(\mathbf{k})] . \quad (8)$$

Finally, we calculate the density of states $DOS(\nu)$ and the real part of the optical conductivity tensor $\sigma_1^{\alpha\beta}(\omega)$ derived from the Kubo formula, as previously used in Refs. [12, 13, 14], as described below,

$$DOS(\nu) = -\frac{1}{\pi} \frac{1}{N} \sum_{\mathbf{k} \in \text{FBZ}} \text{Im} (\text{Tr} [G(\mathbf{k}, \nu + i0^+)]) , \quad (9)$$

$$\sigma_1^{\alpha\beta}(\omega) \propto \frac{1}{N} \sum_{\mathbf{k} \in \text{FBZ}} \left(\int d\nu \left(\frac{f(\nu, T) - f(\nu + \omega, T)}{\omega} \right) \text{Tr} \{ [v_\alpha(\mathbf{k})] [A(\mathbf{k}, \nu)] [v_\beta(\mathbf{k})] [A(\mathbf{k}, \nu + \omega)] \} \right) . \quad (10)$$

Here, ω is photon energy variable, N is the number of \mathbf{k} -points, and $f(\nu, T)$ is the Fermi-Dirac distribution function. Note that we extract only the 2×2 graphene block from the original $(2 + 2M) \times (2 + 2M)$ matrices for use in Equation (10).

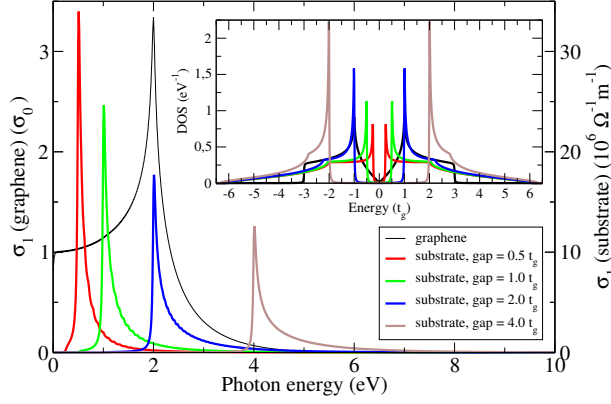


FIGURE 1: The real part of the longitudinal optical conductivity tensor components of free-standing monolayer graphene and each of the bulk substrates. (Inset) The corresponding density of states.

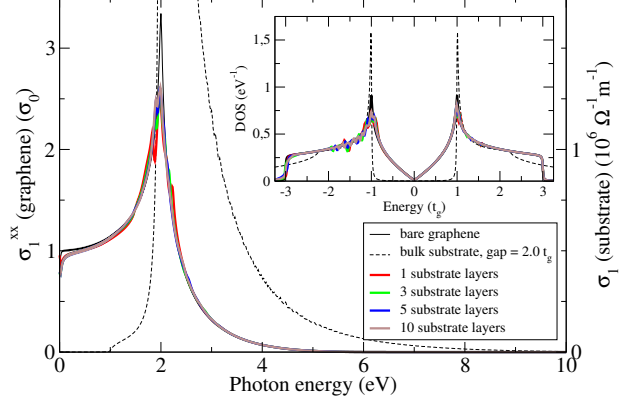


FIGURE 2: The real part of the longitudinal optical conductivity tensor components of the graphene-on-substrate system, with respect to variations in number of substrate layers M , for substrate band gap of $2t_g$ and hybridization strength of 0.1 eV. (Inset) The corresponding density of states.

RESULTS AND DISCUSSION

In our calculations, we arbitrarily choose the hopping parameter for graphene t_g to be 1 eV, and the substrate band gap values to be 0.5, 1, 2, and 4 times t_g . Figure 1 shows the real part of the optical conductivity and the density of states for these bare systems. As these systems are isotropic, the longitudinal optical conductivity tensor components σ_1^{xx} and σ_1^{yy} are identical and nonzero, while the transverse component σ_1^{xy} is zero.

We comment on the number of substrate layers required in the graphene-on-substrate system to be able to mimic the bulk substrate (Fig. 2). Using a higher number of layers increases the size of the Hamiltonian matrix, which in turn increases the computational cost. In our calculations we use 1, 3, 5, and 10 substrate layers, and we found that using less than 10 substrate layers results in a coarser profile. We interpret this as the system undergoing a transition from two to three dimensions with an increasing number of layers.

Generally, hybridization in a system takes two or more distinct energy levels and creates new hybrid levels from those, with each having energies different from the original energy levels through a linear combination. The hybridization is strongest when the original energy levels are similar in energy. Thus, we would like to focus on a substrate energy gap of $2t_g$ first. As shown on the inset of Fig. 2, the peaks of the density of states of monolayer graphene and the bulk substrate model exactly match at energies of $\nu = \pm t_g$. Therefore, when combined into a hybrid graphene-on-substrate system, the effects of the hybridization are strongest, compared to substrates with other energy gap values (Fig. 3). Meanwhile, the effects of the hybridization are weakened for a higher substrate energy gap of $4t_g$.

We note that while the original (bare) monolayer graphene system has a symmetric density of states centered at $\nu = 0$, the density of states of graphene in the hybrid systems lose this symmetry — the new hybrid states, as seen from the fluctuations on the $DOS(\nu)$, are more abundant near $\nu = -t_g$ than $\nu = t_g$. As we increase the strength of the hybridization parameter V , the linear region originally present near the Dirac point in graphene ($|\nu| < 0.3t_g$ for a Dirac point at $\nu = 0$) also starts to skew towards negative energy, therefore increasing the density of states at the Dirac point. We argue that this loss of symmetry is due to the lattice mismatch between the graphene layer and the substrate.

Finally, we make some points on the evolution of the optical conductivity as the hybridization strength is increased (Fig. 4). The peak at photon energy $\omega = 2t_g$ from the bare graphene tends to split into two peaks located at $\omega = 2t_g$ and $\omega = 2t_g - V$, and as the hybridization strength is increased further, the peak at $\omega = 2t_g$ seems to get renormalized to a lower value, distributing its spectral weight to higher energies, as seen from the fluctuations evident in the $2t_g < \omega < 4t_g$ photon energy range. In contrast, the peak at $\omega = 2t_g - V$ begins to rise higher as the hybridization strength parameter is increased. This combination of events results in an apparent redshift of the original unhybridized peak at photon energy $\omega = 2t_g$. Meanwhile, since we hold the Fermi energy of the system at the Dirac point of graphene, the loss of linearity around the Dirac point contributes to a higher value of the DC conductivity.

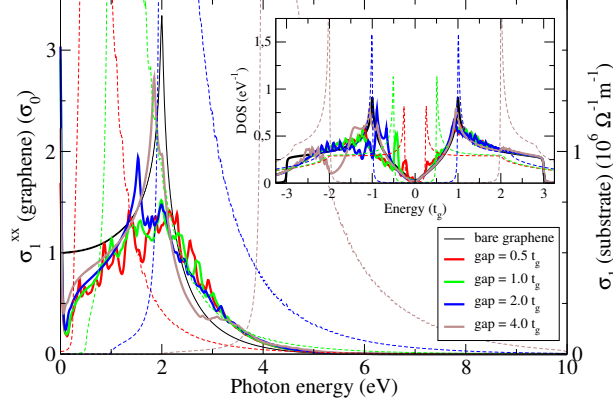


FIGURE 3: The real part of the longitudinal optical conductivity tensor components of the graphene-on-substrate system, with respect to variations in substrate band gap values, for a hybridization strength of 0.4 eV and 10-layer substrates. Dashed lines correspond to bulk substrates. (Inset) The corresponding density of states.

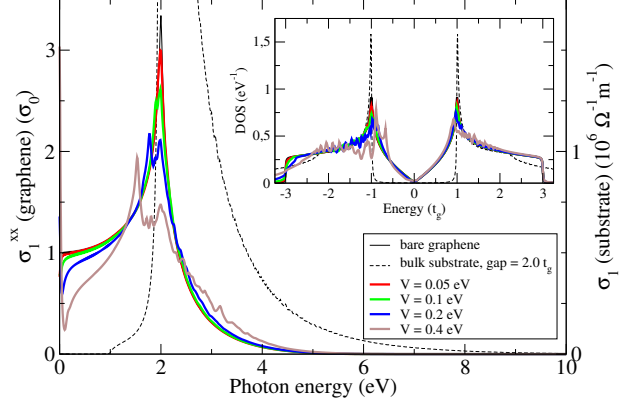


FIGURE 4: The real part of the longitudinal optical conductivity tensor components of the graphene-on-substrate system, with respect to different hybridization strengths, for a 10-layer substrate with a band gap of $2t_g$. (Inset) The corresponding density of states.

CONCLUSION

We have developed, analyzed, and discussed a simple model to investigate hybridization in graphene-on-substrate systems based on the tight-binding approximation. We found that using a 10-layer substrate gives optimal results for our purposes. The resulting density of states $DOS(\nu)$ and the real part of the optical conductivity tensor $\sigma_1^{ab}(\omega)$ of the graphene layer show that the graphene-substrate hybridization tends to renormalize the peak and split it into two peaks, in both the $DOS(\nu)$ and the $\sigma_1^{ab}(\omega)$, most prominently when the substrate band gap is $2t_g$, where t_g is the graphene nearest-neighbor hopping parameter. We also observe in the $DOS(\nu)$ that the hybridization is stronger for $\nu < 0$ than $\nu > 0$, which we propose to be due to the lattice mismatch between the graphene and substrate lattices. Furthermore, the appearance of new hybrid states around the Fermi energy tends to enhance the DC conductivity. Meanwhile, substrates with a higher band gap (around $4t_g$) weaken the effects of the hybridization.

ACKNOWLEDGMENTS

We acknowledge valuable discussions with Shaffique Adam of National University of Singapore.

REFERENCES

1. K. S. Novoselov *et al.*, *Science* **306**, 666 (2004).
2. Y. Z. Zhang *et al.*, *Nat. Commun.* **4**, 1811 (2013).
3. C. H. Liu, Y. C. Chang, T. B. Norris, and Z. H. Zhong, *Nat. Nano.* **9**, 273 (2014).
4. X. H. Cai *et al.*, *Nat. Nano.* **9**, 814 (2014).
5. M. Bernardi, M. Palummo, and J. C. Grossman, *Nano Lett.* **13**, 3664 (2013).
6. J. T. W. Wang *et al.*, *Nano Lett.* **14**, 724 (2014).
7. H. S. Park *et al.*, *Nano Lett.* **14**, 5148 (2014).
8. D. W. Chang, H. J. Choi, A. Filer, and J. B. Baek, *J. Mater. Chem. A* **2**, 12136 (2014).
9. F. Withers *et al.*, *Nat. Mater.* **14**, 301 (2015).
10. V. N. Kotov, B. Uchoa, V. M. Pereira, F. Guinea, and A. H. Castro Neto, *Rev. Mod. Phys.* **84**, 1067 (2012).
11. P. K. Gogoi *et al.*, *Phys. Rev. B* **91**, 035424 (2015).
12. M. A. Majidi, H. B. Su, Y. P. Feng, M. Rübhausen, and A. Rusydi, *Phys. Rev. B* **84**, 075136 (2011).
13. M. A. Majidi *et al.*, *Phys. Rev. B* **87**, 235135 (2013).
14. M. A. Majidi, S. Siregar, and A. Rusydi, *Phys. Rev. B* **90**, 195442 (2014).